Proc. NIPR Symp. Polar Meteorol. Glaciol., 5, 39–55, 1992

DEVELOPMENT OF SHORT-MILLIMETER AND SUB-MILLIMETER WAVE RADIOMETER/SPECTROMETER SYSTEM FOR OBSERVING OZONE AND TRACE GASES IN THE UPPER ATMOSPHERE

Harunobu MASUKO and Satoshi OCHIAI

Remote Sensing Research Section, Applications Division,
Communications Research Laboratory,
2–1, Nukui-Kitamachi 4-chome, Koganei-shi, Tokyo 184

Abstract: Trace gases such as ClO, HO_2, etc. in the upper atmosphere play important roles in the chemistry of the ozone layer. The radiometer/spectrometer system operating in the millimeter and sub-millimeter wave range is the most promising method to remotely observe such upper atmospheric ozone and other trace gases. The system makes it possible to monitor the vertical profiles of the trace gases from the ground. Limb emission observation from space makes it possible to globally estimate the three dimensional distributions of the trace gases. Communications Research Laboratory (CRL) has started to develop a ground-based system operating in the short-millimeter wave range. We are also planning to develop a balloon-borne system, which is necessary for basic estimation of the satellite-borne system and its data analysis. In this report, we present the plan of CRL, together with the results of the feasibility study for developing these systems.

1. Introduction

Recently, the earths environmental problems, such as destruction of the ozone layer and the greenhouse effect, which are caused by man-made products, have increased general concern over the conditions of the upper atmosphere. Especially, observation of the ozone hole in the Antarctic has greatly increased the necessity for accurate measurements of trace gases in the upper atmosphere, such as chlorine monoxide (ClO), which is produced from man-made chlorofluorocarbons (CFC's) and is the main cause of the ozone hole. Until now, upper atmospheric ozone and trace gases have been monitored by measurements of absorption or backscattering of solar ultraviolet or infrared light. In these cases, the observation conditions are restricted and height profiling of the trace gases from the ground is very difficult. On the other hand, spectroscopic measurements in the millimeter and sub-millimeter wave ranges provide an effective mean to monitor the trace gas concentrations together with their height profiles. Especially, the short-millimeter wave radiometer/spectrometer is the only system to measure trace gases such as ClO and HO_2 from the ground (PARRISH *et al.*, 1988). Figure 1 shows the general concept of observations by these systems. In the case of balloon-borne and satellite-borne systems, the observations are made by limb sounding, which makes very sensitive measurement possible (WATER *et al.*, 1984). Especially, the satellite-borne sub-millimeter wave system makes it possible

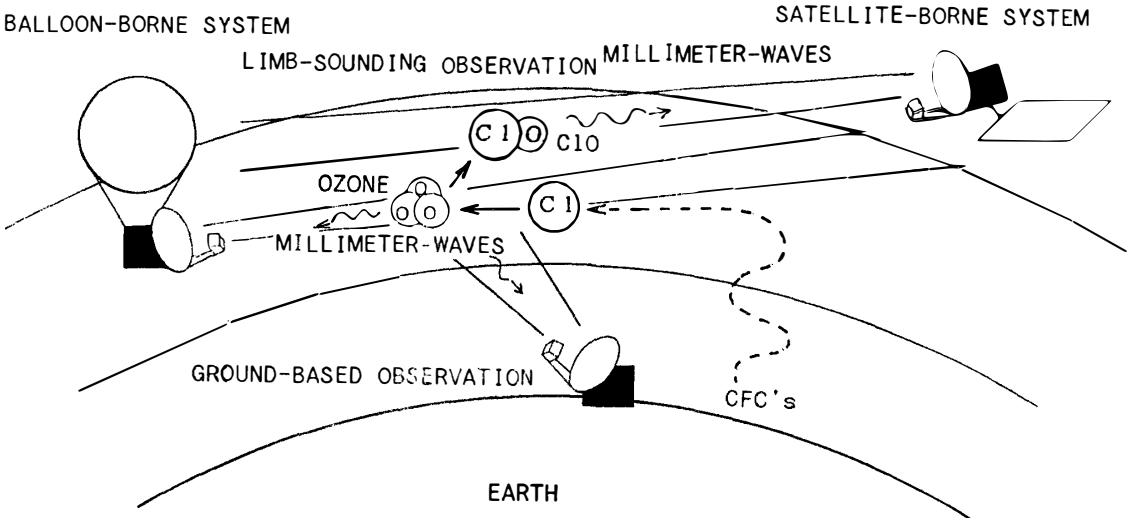

Fig. 1. General concept of observations by short-millimeter and sub-millimeter wave systems.

to accurately measure the global distribution of a wide variety of trace gases with height profiles of excellent vertical resolution (WATER, 1989).

In spite of these advantages, utilization of this method has been limited until now, because the engineering techniques for application of short-millimeter and sub-millmeter waves are very difficult, especially in the field. Communications Research Laboratory (CRL) has started the development of a super short radio wave system to monitor trace gases with high sensitivity based on the recent technological progress. As the first step, we have done several simulated calculations for cases of ground-based observation, and also balloon-borne and satellite-borne limb observations. We report the results of the simulation study and present the CRL plan.

2. Background

Almost all species of atmospheric gases have absorption spectra in the short-millimeter to sub-millimeter wave range due to rotational transitions in the ground state or in the vibrational excited state caused by their electric dipole or magnetic dipole moments. Figure 2 shows examples of the spectra of O_3 ClO and HO_2 in the frequency range up to 1000 GHz. The intensity of each spectral line shows the zenith absorption at the peak, which is calculated based on Liebe's semi-empirical model (LIEBE, 1989), JPL Line Catalogue (POYNTER and PICKETT, 1985) and the U.S. standard atmosphere modified by AFGL (ANDERSON *et al.*, 1986). The excitation energies of the rotational and some of rotation-vibrational states are nearly the same as or less than the thermal kinetic energies of the molecules. This means that the population of the rotational and rotational-vibrational states depends on temperature very weakly. The intensity of emission in the spectral range can be estimated under thermal equilibrium conditions and is expressed by Planck's Radiation Law; it should be remarked that, in the short-millimeter to sub-millimeter wave range above 100 GHz, the Rayleigh-Jeans Approximation Law is not applicable (ULABY *et al.*, 1981). The signal received by the system is calculated by the equation of radiative transfer (WATER,

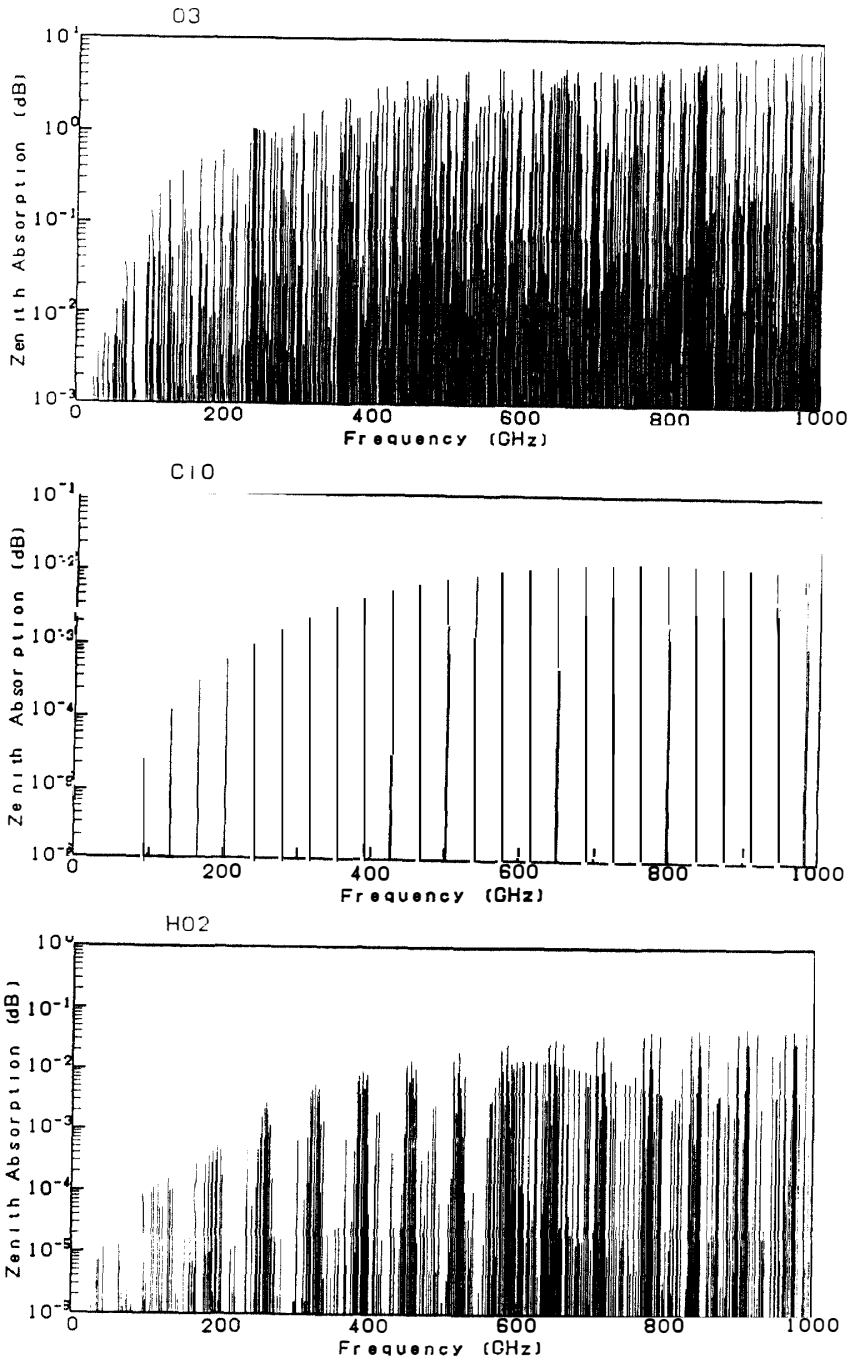

Fig. 2. Spectra of ozone, ClO and HO_2 in the frequency range from 0 to 1000 GHz.

1976):

$$T_A = T_S \cdot \exp\{-\tau_\nu(\infty, 0)\} + \int_\infty^0 K_\nu(s) \cdot T_\nu(s) \cdot \exp\{-\tau_\nu(s, 0)\} \mathrm{d}s \,, \tag{1}$$

where T_A, T_S and T_ν are the antenna temperature, the cosmic radiation temperature and the atmospheric temperature, respectively, expressed by the Rayleigh-Jeans equivalent formula:

$$T_\nu(s)=\frac{h\nu}{k}[\exp\{h\nu/kT(s)\}-1]^{-1}\,. \tag{2}$$

The term related to cosmic radiation temperature (2.74 K) is negligibly small. τ_ν is opacity.

$$\tau_\nu(s', s)=\int_{s'}^{s} K_\nu(r)\cdot \mathrm{d}r\,, \tag{3}$$

K_ν is the sum of the absorption coefficients of all atmospheric gases: $K_\nu=\sum (K_\nu)_{lm}$. The absorption coefficient of a spectral band, $(K_\nu)_{lm}$, is proportional to the number density of molecules, N (mol/cm^3):

$$(K_\nu)_{lm}=I_{lm}(T)\cdot N\cdot\frac{\nu}{\nu_{lm}}\cdot f(\nu, \nu_{lm})\,, \tag{4}$$

ν_{lm} is resonance frequency, and $I_{lm}(T)$ is absorption strength (POYNTER and PICKETT, 1985). N can also be expressed by volume mixing ratio, r_m (ppmv), pressure, p (kPa), and normalized atmospheric temperature, $\theta=300/T$:

$$N=2.41432\times 10^{11}\cdot p\cdot r_m\cdot\theta\,, \tag{5}$$

$f(\nu, \nu_{lm})$ is spectral shape function. The line spectrum is broadened by both thermal collisions of molecules and Doppler velocities. In the case of pressure broadening which gives the principal contribution at altitudes less than 60 km, the spectral band shape is expressed by a Lorenzian function or Gross function for traces gases (ULABY *et al.*, 1981). Both functions give nearly the same shape. The spectral band shapes of H_2O and O_2 are approximated by a modified Van-Vleck-Weiskopf shape function in the altitude range from 0 to 30 km (LIEBE, 1989). Half of the spectral band width in these shape functions, $\Delta\nu$, is expressed by

$$\Delta\nu=\Delta\nu_o\cdot\frac{p}{p_o}\cdot\left(\frac{T}{T_o}\right)^{-x}=a\cdot p\cdot\theta^x\,. \tag{6}$$

The constant "a" and the power "x" for ClO are 0.0255 GHz/kPa and 0.75, respectively (PICKETT *et al.*, 1981), and for ozone, 0.0227 GHz/kPa and 0.77, respectively (CONNOR and RADFORD, 1986). In the altitude range higher than 80 km, Doppler broadening prevails, and the spectral shape is Gaussian (WATER, 1976). $\Delta\nu$ is expressed by

$$\Delta\nu=\frac{\nu_{lm}}{C}\sqrt{\ln 2}\cdot\sqrt{\frac{2kT}{m_o}}=3.58117\times 10^{-7}\cdot\nu_{lm}\left(\frac{T}{M}\right)^{1/2}. \tag{7}$$

At altitudes from 60 to 80km, both pressure and Doppler broadening are effective, and the spectral shape is expressed by a Voigt function which is the convolution integral of a Lorenzian by a Gaussian (BAKSHI and KEARNEY, 1989). Figure 3 shows $\Delta\nu$ of ozone spectral bands. Because Doppler spectral broadening is proportional to frequency, the altitude of the upper boundary of the region where the pressure broadening prevails becomes lower with increasing frequency.

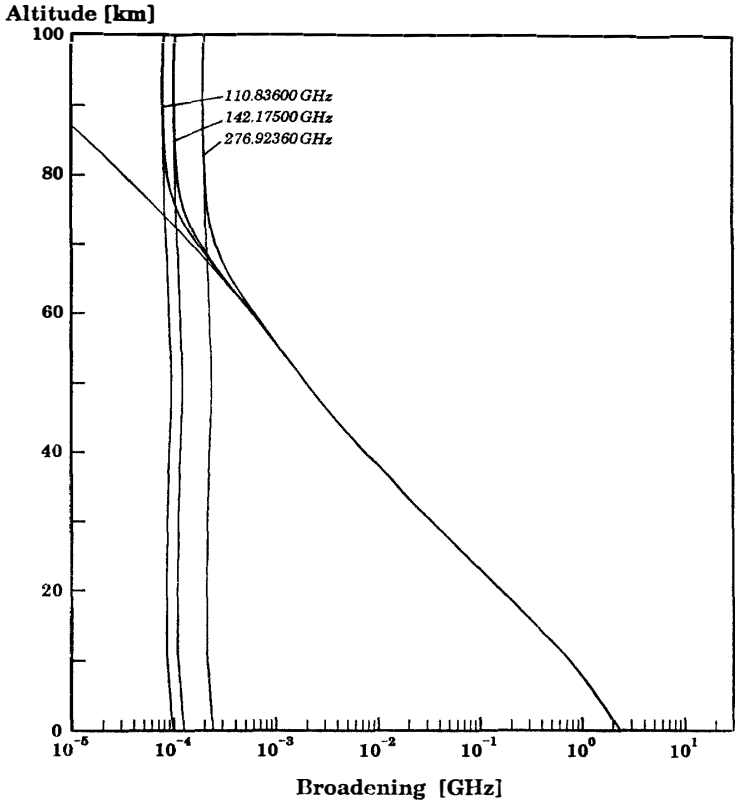

Fig. 3. Contributions of pressure broadening and Doppler broadening of ozone bands expressed by half of the spectral band width as a function of altitude.

3. Simulation Calculations and Results for Ground-Based Observation

The spectral intensities of the trace gases are normally stronger for higher frequency bands, so that it is preferable to use higher frequencies for observation with larger sensitivity. On the other hand, absorption of tropospheric gases, especially water vapor, is very strong in the frequency range above 310 GHz; exceptions are the areas of very low atmospheric water vapor, such as the Antarctic where observations even in the 600 and 800 GHz bands are possible. Therefore, for ground-based observation of trace gases, it is preferable to use the spectral bands in the 200–310 GHz region between the strong H_2O bands at 183.310 and 325.153 GHz. This window region is wide and the back-ground absorption level is comparatively flat. Furthermore, there are many spectral bands of important trace gases in the window region. Figure 4 shows examples of calculations for ground-based observations of the 276.923 GHz ozone band and 278.63 GHz ClO bands based on eqs. (1) to (5). The 276.923 GHz band is preferable to accurately observe ozone, because the temperature dependence is a minimum for the rotational transition and accuracy of the height profile of atmospheric temperature is not critical for retrieving ozone profiles (CONNER *et al.*, 1987). The 278.63 GHz bands are the most intense ClO bands in the window region.

To retrieve the height profiles of ozone or other trace gases from the measured antenna temperature spectrum, we utilize the pressure broadening of the spectral bands. Pressure in the upper atmosphere can easily be related to height. Using eqs. (4),

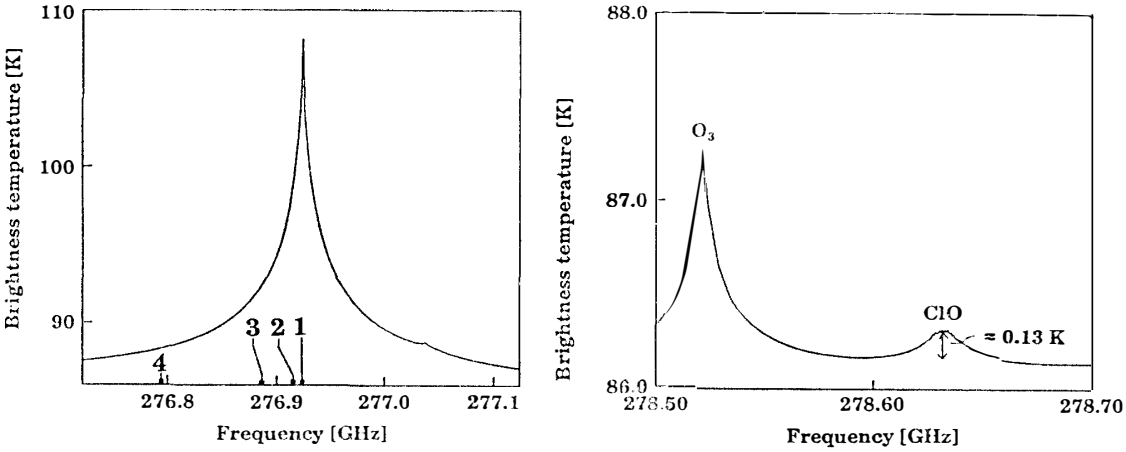

Fig. 4. Expected spectral band of ozone (left) and ClO (right) for ground-based observations at the mountain top of 4000 m and elevation angle of 20 degrees.

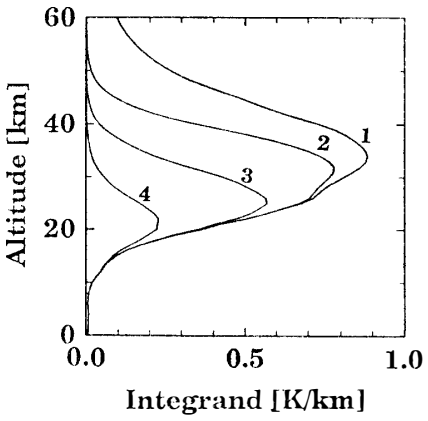

Fig. 5. Integrand functions of ozone based on the number-density height profile in the AFGL Table (ANDERSON et al., 1986). Each integrand is for the frequency position numbered in the ozone band of Fig. 4.

the equation of radiative transfer (1) is written as

$$T_{A\nu}=\int_{\infty}^{0} N(Z)\cdot W(\nu, Z)\mathrm{d}Z\ , \tag{8}$$

where $W(\nu, Z)$ is a number-density weighting function. Figure 5 shows an example of the integrand, $W(\nu, Z)\cdot N_o(Z)$, for ozone, where $N_o(Z)$ is a typical number-density height profile; the true profile is expressed by $N(Z)=N_o(Z)\cdot N'(Z)$, where $N'(Z)$ is the deviation from the assumed profile. The integral eq. (8) can be approximated by the following matrix equation:

$$\begin{bmatrix} T_{A\nu_1} \\ \vdots \\ T_{A\nu_n} \end{bmatrix} = [W(\nu_i, Z_j)\cdot \Delta Z]_{\substack{i=1,n \\ j=1,m}} \cdot \begin{bmatrix} N(Z_1) \\ \vdots \\ N(Z_m) \end{bmatrix} \tag{9}$$

$N'(Z)$ can be calculated by the following inverse matrix:

$$[N'(Z_j)]_{j=1,m}=[\{[W_{ij}\cdot N_{oj}]^t\cdot[W_{ij}\cdot N_{oj}]\}^{-1}\cdot[W_{ij}\cdot N_{oj}]^t\cdot \Delta Z^{-1}]_{\substack{i=1,n \\ j=1,m}}\cdot[T_{A\nu_i}]_{i=1,n}\ . \tag{10}$$

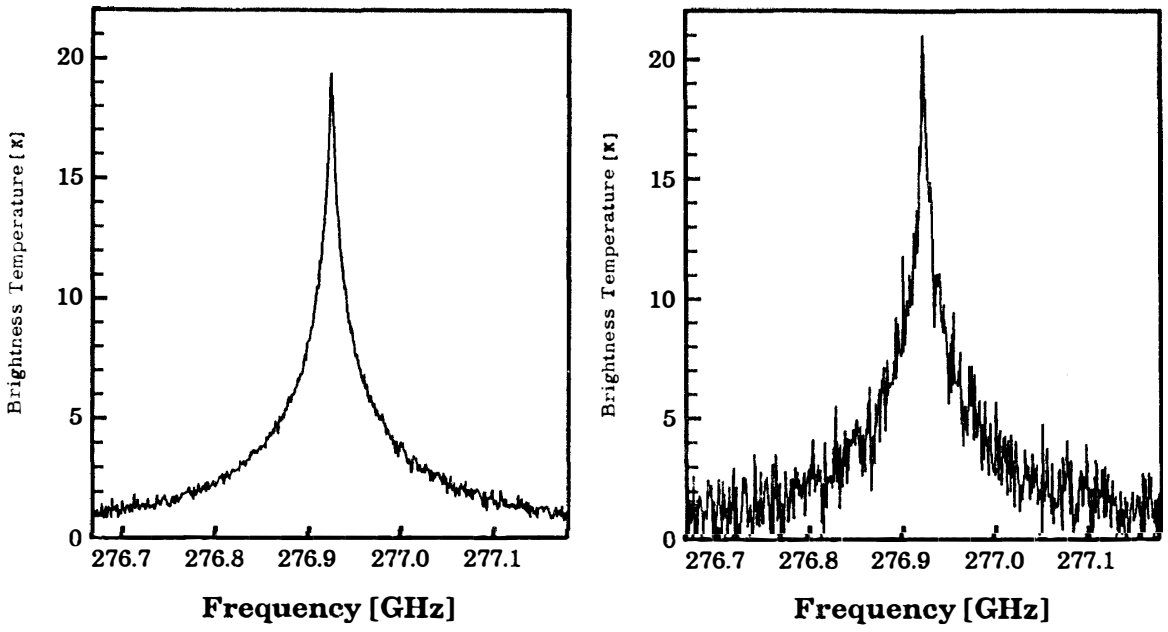

Fig. 6. Simulated brightness temperature spectra for the 276.923 GHz ozone bands at altitude of 4 km and for antenna elevation angle of 20 degrees. The total band width is 512 MHz, and resolution is 1 MHz. The left-hand and right-hand figures show the case of the mean of added random noise of 1% and 5% of the peak intensity, respectively, which correspond to the integration time of 21 and 0.8 s for a total-power receiver with the system noise temperature of 800 K, respectively.

This gives the solution of the least-square equation. In general, eq. (10) is not suitable when measured values include errors. In order to obtain an optimal solution, several inverse methods have been tried (TWOMEY, 1977). In our simulation calculation, both the modified Chahine method proposed by Twomey and the Backus-Gilbert method are tested together with the least-square method. The modified Chahine method gives a comparatively good result. Therefore, based on the modified Chahine method, we estimated the relationship between receiver sensitivity and retrieved profile error, which corresponds to the observation error. The estimate is made by simulating the antenna temperature spectrum by adding receiver noise. Figure 6 shows examples of the simulation calculations for the 276.923 GHz ozone band. According to the estimate, observation within an error of 10% requires receiver sensitivity to be less than 2% of the peak intensity of the observed band. The sensitivity of the radiometer receiver of zero-balanced Dicke type is expressed by the following equation:

$$\Delta T = \frac{2(T_{SYS} + T_A)}{\sqrt{B\tau}}, \tag{11}$$

where T_{SYS} means system noise temperature; B is channel band width; τ is integration time. The factor 2 on the right-hand side of the equation should be eliminated in the case of a total-power radiometer which can be used in balloon-borne or satellite-borne systems.

If we assume a total-power receiver with T_{SYS} of 800 K, which can at present be

achieved by a semiconductor diode mixer cooled to 20 K (PARRISH *et al.*, 1988), the example of the left-hand side in Fig. 6 corresponds to the integration time of 21 s and that of the right-hand side of the figure is 0.8 s. Therefore, for ozone, a few minutes of observation is enough to obtain a height profile with error of less than 10%. On the other hand, for the observation of ClO shown in Fig. 4, the sensitivity must be a few milli-Kelvin in order to attain the desired accuracy, and the integration time becomes a few tens of hours under the above-mentioned conditions. Observation of upper-atmospheric trace gases requires a noise receiver with much lower noise, such as one using a super-conductor mixer. Furthermore, the observation should be made under very low water vapor pressure, such as on top of a high mountain or in the polar regions. If these conditions can be fulfilled, the integration time can be decreased up to several hours. In this case, we can make reliable observations of the diurnal variation of trace gases.

4. Simulation Calculations and Results for Balloon-borne and Satellite-borne Observations

Limb-sounding observation offers several advantages because of viewing geometry (ULABY *et al.*, 1986; WATER 1989). It provides the largest possible signals from the trace gases due to the long observation path length along the tangential line of sight. Figure 7 shows examples of simulation calculations for balloon-borne limb-sounding observations in the 276.923 GHz ozone band and the 278.63 GHz ClO bands. In both cases, the peak intensities become much larger than in the cases of ground-based observations. In each spectrum, the influence of the emissions from the altitude range below the tangential line of sight is very slight, and that from the altitude range above the tangential line of sight is weakened because of the shorter observation path lengths; for almost all trace gases, a large part of weighting function is in the altitude range illuminated by antenna beam. Due to this condition, high vertical resolution, *e.g.* 2 km, can be achieved in the limb-sounding observation. Figure 8 shows an example of the vertical weighting function for limb observation of the ozone

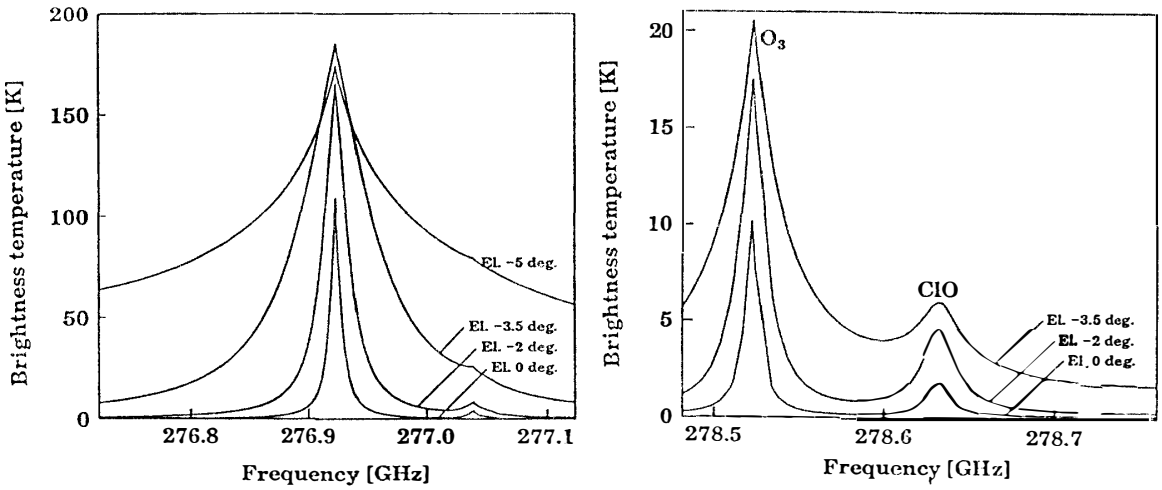

Fig. 7. Expected spectral band of ozone (left) and ClO (right) for balloon-borne limb-sounding observation at the latitude of 40 km.

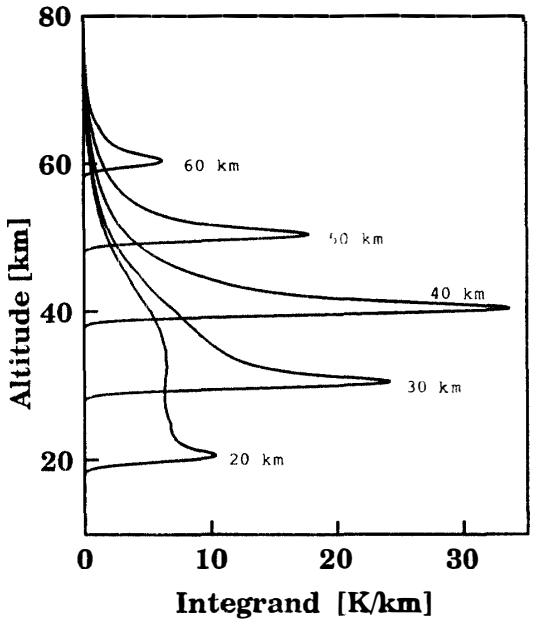

Fig. 8. Limb-weighting functions of the ozone 276.924 GHz band for a 1.5 km antenna beam footprint at the tangent point. The numbers in the figure show the tangent height.

band. To obtain height profiles, the limb emission of each tangent height is observed by vertical scanning of the narrow beam antenna. By combining the results of the above-mentioned inverse analysis for the spectral data obtained at each tangent height, we can obtain sufficient observation accuracy even with less receiver sensitivity; the integration time can be greatly shortened by limb-sounding observation. A disadvantage of the limb-sounding observation is low horizontal resolution along the line of sight. The half widths are generally larger than a few hundred kilometers.

Furthermore, in the limb-sounding observation, bands in the sub-millimeter wave range are available because of the very low density of water vapor in the upper atmosphere; while, ozone bands become obstacles for observing trace gas constituents because of their strong intensities and comparatively large densities. Considering the frequency range below 800 GHz, which can be used on the basis of the present hardware limitation as mentioned below, the bands around 635 GHz is preferable to cover almost all species of the trace gases related to ozone chemistry. Table 1 shows examples of the suitable frequency bands of upper atmospheric trace gases to be monitored. The bands around 560 GHz are also listed in the table based on the consideration by WATER (1989). To estimate the preferable frequencies for a satellite system, we evaluate the performance of the cases operated around 270 and 635 GHz based on the present engineering level. Table 2 shows the parameters used in the evaluation; the altitude of the satellite is 800 km; the antenna diameter is 1 m. Normal semiconductor diode mixers cooled at 20 K are assumed for both frequencies. Figure 9 shows the geometry of the satellite limb sounding and the performance of antenna scanning. The observation is made in the height range from 14 to 80 km at intervals of 2 km. Calibrations with hot and cold sources are done at the lowest and highest positions, respectively. The integration time at each position is 0.25 s. The antenna beam is assumed to be scanned step by step in 0.05 s. One round-trip scan of the antenna beam is defined as one sequence.

Table 1. Suitable frequency bands for observing trace gases and physical quantities in the upper atmosphere.

Species	<200 GHz	205 GHz bands	270 GHz bands	560 GHz bands	635 GHz bands	Other bands	Comments
O_3		206.132	276.923	566.294	623.688	651.475	Many bands
^{18}OOO							TBD
$O^{18}OO$							TBD
^{17}OOO							TBD
$O^{17}OO$							TBD
^{35}ClO		204.35	278.63	575.39	649.45		
^{37}ClO							TBD
ClO_2					624.269		Insufficient data
$HO^{35}Cl$		202.485	270.832		635.870		
$HO^{37}Cl$							TBD
$ClONO_2$							Low intensity
$H^{35}Cl$					625.92		
$H^{37}Cl$					624.98		
$CH_3{}^{35}Cl$							Insufficient data
$CH_3{}^{37}Cl$							Insufficient data
^{79}BrO		218.0		576.30	627.37	652.88	Many bands near 600 GHz
^{81}BrO				573.92	624.77	650.18	Many bands near 600 GHz
$H^{79}Br$				500.647			
$H^{81}Br$				500.497			
OH						1834.74	Far-infrared region
H_2O		183.310		556.936		380.197	
HO_2			265.770	569.390	625.660	641.643	Many bands near 600 GHz
H_2O_2		204.575	270.610	571.854		599.723	
HDO				559.817	622.482	599.926	
HNO_3				544.350			TBD
HO_2NO_2					651.5		Insufficient data
NO			250.437	551.2/5	651.4/8		
NO_2		215.26	274.96	578.2/4	647.22		
N_2O			276.328	557.578	627.752		
N_2O_5							Insufficient data
HCN			265.886		620.304		
SO_2		204.246	275.240	559.500	641.825		Many bands
OCS		206.745	267.530	558.990	643.863		Many bands
CO		230.537		576.268			
H_2CO		211.211	281.526	561.900	631.705		
Temp. (O_2)	60 GHz bands	118.750				368.490	
Press. (O_2)	60.00					63.57	
Wind (O_2)							Better in visible
Liquid water							H_2O-bands + background

Table 2. Parameters used in evaluation of the satellite-borne limb-sounding system.

Parameter	Assumptions	Condition/Comments
Satellite altitude	800 km	
Satellite velocity	7.6 km/s	
Antenna diameter	1 m	Elevation direction
Instantaneous field of view at tangent point	3.5 km	276–279 GHz
	1.5 km	625–650 GHz
Receiver total noise power for DSB	800 K	276–279 GHz
	4000 K	625–650 GHz
Spectral resolution	2 MHz	
Observation height	14–80 km	
Antenna scanning	2 km step	Number of steps: 34
Scanning width of depression angle	25.90–27.09°	Scanning angle: 1.19°
Interval of antenna scanning	0.36°	

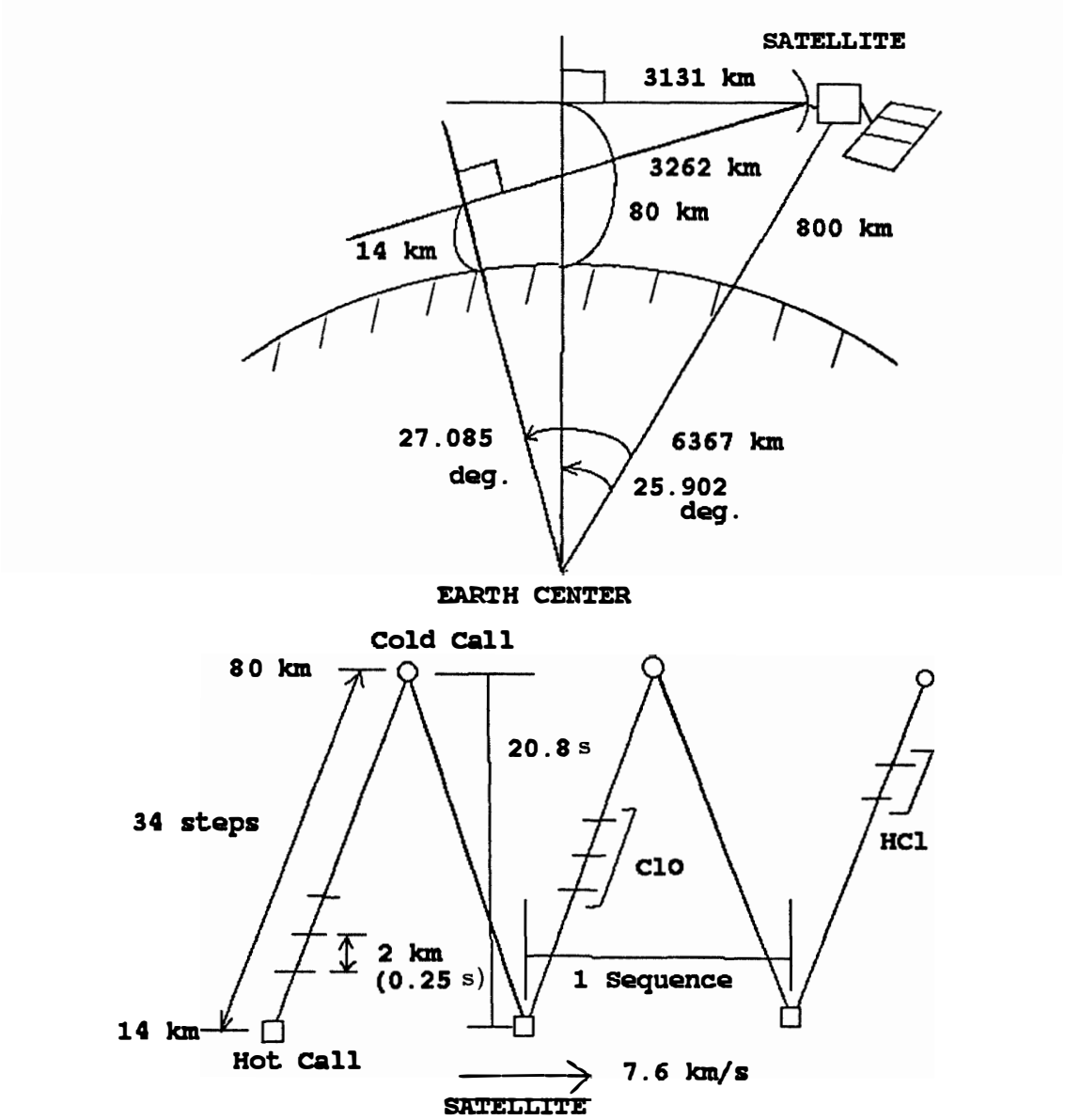

Fig. 9. Geometries of the satellite limb-sounding and the antenna scanning assumed in the evaluation study.

Table 3. Results of the evaluation study for the satellite-borne limb-sounding system.

	276–279 GHz			625–650 GHz		
	O_3	ClO	N_2O	O_3	ClO	HCl
Observation unit (sequence)	2	6	4	2	2	2
Vertical resolution (km)	3.5	5.5	3.5	1.5	3.8	1.5
Data sampling (km)	2	2	2	2	2	2
Observation height range (km)	16–80	18–50	12–50	16–80	16–50	16–60
Expected peak intensity (K)	10–200	2–5	20–50	10–200	10–20	50–100
Accuracy (K)	0.71	0.23	0.43	3.0	1.4	1.45
Integration time (s)	1	6	2	1	4	4
Resolution along the line of sight (km)	300–400					
Azimuth resolution (km)	316	948	632	316	632	632

Table 3 shows the results of the estimation. In this method, the vertical resolution is affected both by the instantaneous field of view, which is better for the 635 GHz band than for the 270 GHz band, and by the integration time, which is shorter for the former than for the latter. The integration time also affects the horizontal resolution related to the satellite motion. From the viewpoint of atmospheric science, HCl, which is one of the important species related to the chlorine cycle, can be observed at 625 GHz. Furthermore, the assumed mixer performance in the sub-millimeter wave range will be possibly improved in the near future. Therefore, we can conclude that the 635 GHz band are better than the 270 GHz band for satellite observations of the trace gases.

5. Heterodyne Radiometer and Spectrometer System

The heterodyne radiometers and spectrometers considered here have been developed and used for a long time in the field of radio astronomy (PAYNE, 1989). The astronomers observe emissions from interstellar gases by millimeter or sub-millimeter wave radio telescopes. The system performance is nearly the same as that used for earth environment research. Figure 10 shows the schematic diagram of a typical short-millimeter or sub-millimeter wave heterodyne radiometer and spectrometer. The signals received by an antenna are guided to heterodyne receivers through quasi-optical paths. Along the paths, signals of different frequency bands are divided by diplexers or beam splitters. For a ground-based system, a Dicke switching mechanism may also be set along the quasi-optical paths. A diplexer such as a Folded-Fabry-Perot type interferometer is used to combine the received signal with the signal from a local oscillator (LO). A solid-state LO is used because of its high reliability and stability. However, at the present stage, the solid-state LO is only available in the frequency range below about 130 GHz. Therefore, a frequency multiplier is used to obtain the LO power in the short-millimeter to sub-millimeter wave range. Because of very low output power of the frequency multiplier, multiplying less than 6 times

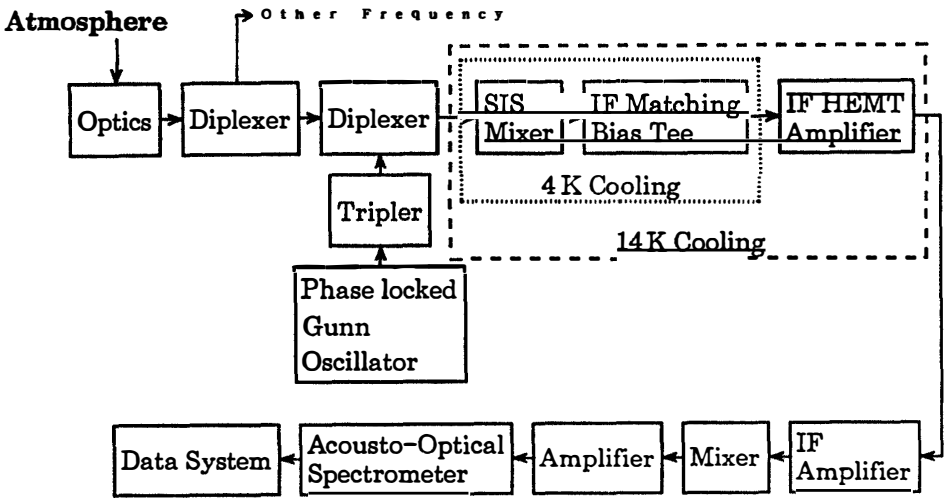

Fig. 10. Schematic diagram of short-millimeter or sub-millimeter wave heterodyne radiometer and spectrometer system.

is only available for practical systems. As a result, at our present engineering level, the available frequencies for a reliable system are less than 800 GHz. The RF frequency is directly fed to a low-noise mixer, which coherently convert the received frequency to the difference frequency (IF frequency) from the LO frequency. Normally, the IF frequency is in microwave range, from the L band to the Ku band, which can be highly amplified by a low-noise amplifier. The system noise temperature, T_{SYS}, is roughly determined in the stage up to the first IF amplifier:

$$T_{SYS}=T_M+L\cdot T_{IF}\,, \tag{12}$$

T_M and T_{IF} are noise temperatures of the mixer and IF amplifier, respectively. L is the mixer conversion loss. Therefore, a highly sensitive system requires a mixer with both low noise and low conversion loss. Such conditions are achieved by a superconductor mixer. Especially, a superconductor-insulator-superconductor (SIS) mixer is the best one for use in the millimeter to sub-millimeter wave range. At the present stage, however, few SIS mixers are used in practical systems with frequency range larger than 200 GHz because of the engineering difficulty.

A disadvantage of the superconductor system is cooling to 4 K, which in general make the system large and complicated. A low-noise IF amplifier, such as a high electron mobility transistor (HEMT), is also used under cooling conditions. After further amplification and frequency conversion at room temperature, the signal is guided to a spectrometer. Several types of spectrometer are potentially available: filter bank spectrometer (FBS), acousto-optical spectrometer (AOS), surface acoustic wave spectrometer (SAWS), fast Fourier transformation spectrometer (FFTS), and correlation spectrometer (CS). The former 3 types are analog-type spectrometers, and the latter 2 types use digital signal processing. The FBS is primitive, heavy and expensive. At the present stage, digital spectrometers are still under development because of the difficulties of ultra fast digital signal processing and VLSI technology. SAWS also requires ultra fast digital signal processing. Therefore, at present, AOS

is preferable. Furthermore, AOS is not so expensive and has excellent reliability and possibility of wide-band operation.

6. Plans of CRL

In 1990, CRL started to develop a short-millimeter/sub-millimeter wave radiometer/spectrometer system for monitoring trace gases in the upper atmosphere. Figure 11 shows the schedule. In the first three years starting from 1991, a ground based system operating around 204 and 279 GHz is developed to simultaneously observe ozone and ClO. The 279 GHz channel can be used to observe other trace gases, such as HO_2, H_2O_2, HCN, N_2O, etc. (PARRISH *et al.*, 1988). From 1994, observations using the completed system will be started not only in Japan but also in the Antarctic and possibly in the Arctic. SIS mixers and low-noise HEMT amplifiers operating in the C band are combined for highly sensitive detection, short integration time and capability of wide-band observation. We have already started development of SIS mixers operating in these bands in collaboration with Nobeyama Radio Observatory, the National Astronomical Observatory of Japan. A closed-cycle refrigerator is used for simple and stable operation. We are also planning to develop compact-sized AO spectrometers with resolution of 1 MHz and band width of 1 GHz, in which recently developed semiconductor lasers operating in the visible range will be used. The whole system is compact in size and light in weight for easy transportation.

From 1994, we will also develop a balloon-borne system to estimate the basic performance of a satellite-borne system, such as preferable frequencies, detection band width, resolution band width, integration time, detection capability of each trace gas constituent, measurement capability of height profiles, accuracy of observations, etc. Another purpose of the system is to develop data analysis algorithms for the

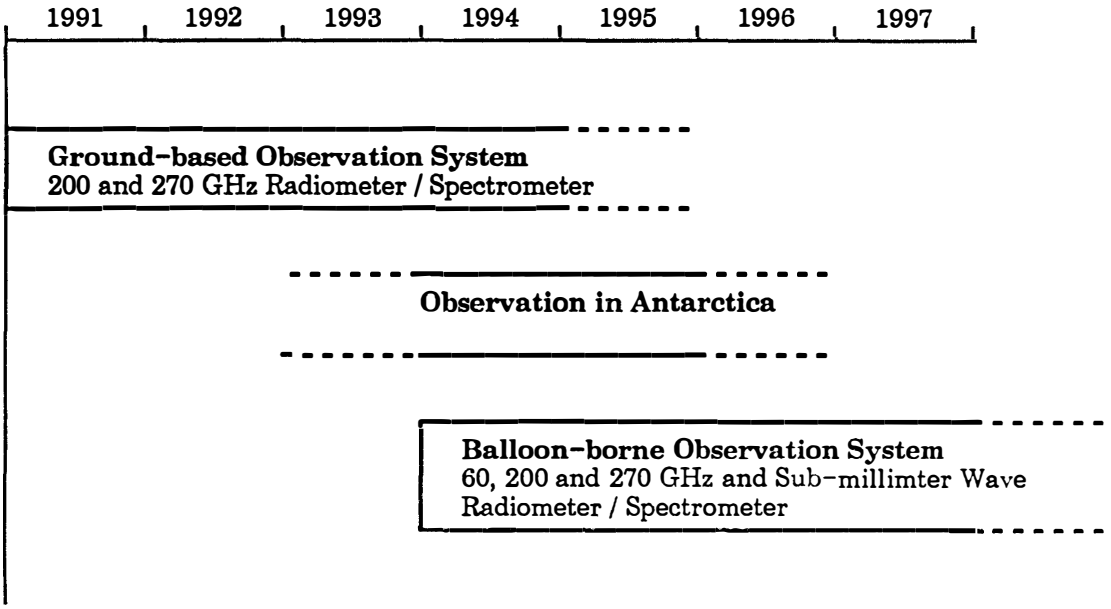

Fig. 11. Schedule of CRL to develop ground-based and balloon-borne short-millimeter and sub-millimeter wave systems.

satellite-borne limb-sounder. The system can also be used for verification and calibration experiments for the satellite system. Furthermore, the balloon-borne system is effective for a short-term campaign experiment, such as those made for observing ozone holes in the Antarctic and in the Arctic. The performance of the balloon-borne system has not been determined yet, but the use of sub-millimeter wavelengths will positively be considered for the future satellite-borne system "MILES (Millimeter-wave Limb Emission Spectrometer)" proposed in the Japanese EOS program, in which frequencies from 60 to 635 GHz will be used. The proposal has been adopted by NASDA (National Space Development Agency of Japan) as a candidate to be one of the sensors mounted on the Japanese low-inclination orbit platform or the second Japanese polar orbit platform (JPOP-2) with high priority. These platforms are planned to be launched in 2000 and 2003, respectively.

7. Conclusions and Remarks

Emission spectro-radiometry in the short-millimeter and sub-millimeter wavelength range has certain advantages to remotely monitor ozone and other trace gases in the upper atmosphere;

First, many kinds of the trace gases have spectral bands in the short-millimeter to sub-millimeter wavelength range, where the overlapping of the bands is not serious and the influence of the strong spectral bands of major atmospheric constituents such as H_2O are comparatively weak.

Second, reliable information on spectroscopic characteristics of the bands can be obtained from comparatively simple calculations without considering excited electronic or vibrational wave functions.

Third, the very high sensitivity of the heterodyne detection system makes it possible to observe the very weak bands of the trace gases.

Fourth, the very high spectral resolution (less than 1 MHz: 0.000033 cm^{-1}) makes it possible to measure vertical profiles of the trace gases from the ground using the pressure broadening of the spectral lines.

Fifth, accurate measurements of atmospheric temperature are not needed because of the weak dependence of the emission bands on temperature.

Sixth, emission spectroscopy makes day/night observation possible.

Seventh, the observations are not affected by aerosols or ice clouds.

Eighth, satellite limb sounding makes it possible to obtain global three-dimensional distributions of trace gases with high accuracy.

For ground-based observations, the system operating around 270 GHz is preferable because of the many related spectral bands and comparatively low influence of tropospheric water vapor in the frequency range. To measure the vertical profiles of the trace gases with accuracy less than 10% and reasonable measurement time, we must develop a very low noise receiver using an SIS mixer and HEMT amplifier cooled to 4 K. CRL has started to develop a compact-size radiometer/spectrometer system with such performance operating at 204 and 279 GHz to simultaneously observe ozone and trace gases from the ground. The system can be used to investigate the roles of trace gases in ozone layer destruction and to monitor diurnal variations,

seasonal variations and long trends of the trace gases not only in Japan but also in the Antarctic and Arctic.

For limb-sounding observations, the bands in the sub-millimeter wavelength range are preferable, because almost all trace gases have spectral bands with strong intensity in the range. From the viewpoints of present technical level and the possibility to monitor HCl, the bands around 635 GHz are suitable. High altitude resolution is also possible using a small-size antenna. A low noise system is also needed because of the short integration time imposed by vertical antenna scanning. Therefore, a cooled semiconductor mixer or SIS mixer are preferable as in a ground-based system. CRL also has a plan to develop a low-noise balloon-borne system to perform basic investigations of the satellite limb-sounding technique. A satellite-borne system "MILES" has been proposed for the first Japanese low-inclination platform (launch: 2000) or the second JPOP (launch: 2003). Frequencies of 60–640 GHz are considered in this proposal.

Acknowledgments

We thank Prof. J. INATANI and Dr. M. TSUBOI of National Radio Observatory and Prof. T. HASEGAWA and Dr. M. HAYASHI of University of Tokyo for their advice in estimating the system performance.

References

ANDERSON, G. P., CHEWYND, J. H., CLOUGH, S. A., SHETTLE, E. P. and KNEIZYS, F. X. (1986): AFGL atmospheric constituent profiles (0–120 km). AFGL-TL-86-0110.

BAKSHI, V. and KEARNEY, R. J. (1989): New tables of the Voigt function. J. Quant. Spectrosc. Radiat. Transfer, **42**, 111–115.

CONNER, B. J. and RADFORD, H. E. (1986): Pressure broadening of millimeter-wave ozone lines by atmospheric gases. J. Mol. Spectrosc., **117**, 15–29.

CONNER, B. J., BARRETT, J. W., PARRISH, A., SOLOMON, P. M., DE ZAFRA, R. L. and JARAMILLO, M. (1987): Ozone over McMurdo Station, Antarctica, austral spring 1986: Altitude profiles for the middle and upper atmosphere. J. Geophys. Res., **92** (D11), 13221–13230.

LIEBE, H. J. (1989): MPM—An atmospheric millimeter-wave propagation model. Int. J. Infrared Millimeter Waves, **10**, 631–650.

PARRISH, A., DE ZAFRA, R. L., SOLOMON, P. M. and BARRETT, J. W. (1988): A ground-based technique for millimeter wave spectroscopic observations of stratospheric trace constituents. Radio Sci., **23**, 106–118.

PAYNE, J. M. (1989): Millimeter and submillimeter wavelength radio astronomy. Proc. IEEE, **77**, 993–1017.

PICKETT, H. M., BRINZA, D. E. and COHEN, E. A. (1981): Pressure broadening of ClO by nitrogen. J. Geophys. Res., **86** (C8), 7279–7282.

POYNTER, R. L. and PICKETT, H. M. (1985): Submillimeter, millimeter, and microwave spectral line catalogue. Appl. Opt., **24**, 2235–2240.

TWOMEY, S. (1977): Introduction to the Mathematics of Inversion in Remote Sensing and Indirect Measurements. Amsterdam, Elsevier, 115–184.

ULABY, F. T., MOORE, R. K. and FUNG, A. K. (1981): Microwave Remote Sensing, Active and Passive, Vol. I, Microwave Remote Sensing Fundamentals and Radiometry. London, Addison-Wesley, 186–343.

ULABY, F. T., MOORE, R. K. and FUNG, A. K. (1986): Microwave Remote Sensing, Active and Pas-

sive, Vol. III, From Theory to Applications. Dedham, Artech House, 1379–1389.

WATER, J. W. (1976): Absorption and emission by atmospheric gases. Methods of Experimental Physics, Vol. 12, Astrophysics, Part B: Radio Telescopes, ed by M. L. MEEKS. New York, Academic Press, 142–176.

WATER, J. W. (1989): Microwave limb-sounding of Earth's upper atmosphere. Atmos. Res., **23**, 391–410.

WATER, J. W., HARDY, J. C., JARNOT, R. F., PICKETT, H. M. and ZIMMERMANN, P. (1984): A balloon-borne microwave limb sounder for stratospheric measurements. J. Quant. Spectrosc. Radiat. Transfer, **32**, 407–433.

(*Received January 23, 1991; Revised manuscript received May 23, 1991*)